Available online at www.sciencedirect.com

SCIENCE DIRECT®

International Journal of Solids and Structures 41 (2004) 6745–6758

INTERNATIONAL JOURNAL OF SOLIDS and STRUCTURES

www.elsevier.com/locate/ijsolstr

Response of a finite beam in contact with a tensionless foundation under symmetric and asymmetric loading

Yin Zhang, Kevin D. Murphy *

Department of Mechanical Engineering, University of Connecticut, 191 Auditorium Road, Storrs, CT 06269-3139, USA

Received 9 May 2004

Abstract

In this work a general analytical model is developed for the static response of a beam resting on a tensionless elastic foundation subjected to a lateral point load. This load may either be located at the center of the beam or may be offset. An analytical/numerical solution is obtained to the governing equations; this solution makes no assumption about either the contact area or the kinematics associated with the transverse deflection of the beam. This is in contrast to previous work in which, for an infinite beam (where the load is symmetric by definition), implicit assumptions about the contact area and the response kinematics were made. Because these assumptions are dropped, the contact behavior differs in several fundamental ways from its infinite counterpart. Specifically, it is shown that (i) the contact area is a sensitive function of the beam length and that this function may change nonmonotonically, (ii) the contact area may depend on the magnitude of the load, (iii) asymmetric loads, which cannot exist in the infinite problem, have a dramatic influence the contact area for the finite system. These features are demonstrated with specific examples and explained in terms of the fundamental physics of the system. The implications for these behaviors are also discussed.

Keywords: Contact; Tensionless foundation

1. Introduction

One common approach to modeling contact behavior is to replace one of the contacting components (presumably the less important one) with an elastic foundation. This approach has the benefit of incorporating the flexibility of the secondary component while greatly simplifying the analysis. This approach has been used repeatedly in the study of beams and plates in contact with other bodies. For example, see Hetenyi (1946) and Timoshenko (1961), which highlight much of the early work on this subject.

The most common beam-foundation model (regardless of whether it is of the Winkler or Reissner variety) allows for both compressive and tensile stresses to exist across the interface between the beam and

* Corresponding author. Tel.: +1-860-4864109; fax: +1-860-4865088.
E-mail address: kdm@engr.uconn.edu (K.D. Murphy).

doi:10.1016/j.ijsolstr.2004.05.028

the foundation. In other words, if a downward lateral load is applied to a beam resting on a foundation, the beam will be compressed into the foundation. If the direction of the load is reversed, the beam and the foundation are pulled up, creating tension in the foundation. However, in applications where adhesion between the beam and the substrate is not assured, this latter behavior is physically unrealistic. Instead, a more appropriate model would be a foundation which reacts to compressive stresses but is incapable of experiencing tension. Such foundations are termed *one-way* or *tensionless* foundations.

Previously, studies on infinite beams in contact with tensionless elastic foundations or semi-infinite substrates have yielded a variety of general results, which are commonly associated with these systems, see Tsai and Westmann (1967), Weitsman (1970, 1971, 1972), and Lin and Adams (1987). However, as it turns out, many of these results occur because of the ‘‘infinite beam’’ assumption. More specifically, they stem from the symmetry that naturally arises; because the beam is infinite, any applied point load must be centered on the beam. So what are these results? To explain, consider the schematic beam-foundation system shown in Fig. 1a. As a load is applied, a portion of the beam is compressed into the substrate; outside the contact zone the outer edges ‘‘lift-off’’ from its zero load equilibrium position. This lift-off condition *must* always occur, regardless of the magnitude of the applied load. This lift-off condition produces another interesting feature. As greater loads are applied, the central portion of the beam plunges deeper into the foundation. However, the outer edges of the plate experience greater lift-off. The result is that the contact area remains constant. Moreover, the contact area is independent of the magnitude of the applied load. All of these general conclusions arise from infinite geometry of the beam and manifest themselves mathematically in the symmetry of the solution to the equilibrium problem.

More recent work has been undertaken on finite structures; these have largely focused on developing new techniques for determining the contact area. Most notably, penelty methods and inequality contraints have been used to determine the contact area (Akbarov and Kocaturk, 1997; Ascione and Grimaldi, 1984; Ascione and Olivito, 1985). Contact and compatibility contraints have also been used to determine the contact zone in nonlinear tensionless contact (Joo and Kwak, 1986). In an interesting twist, Khathlan

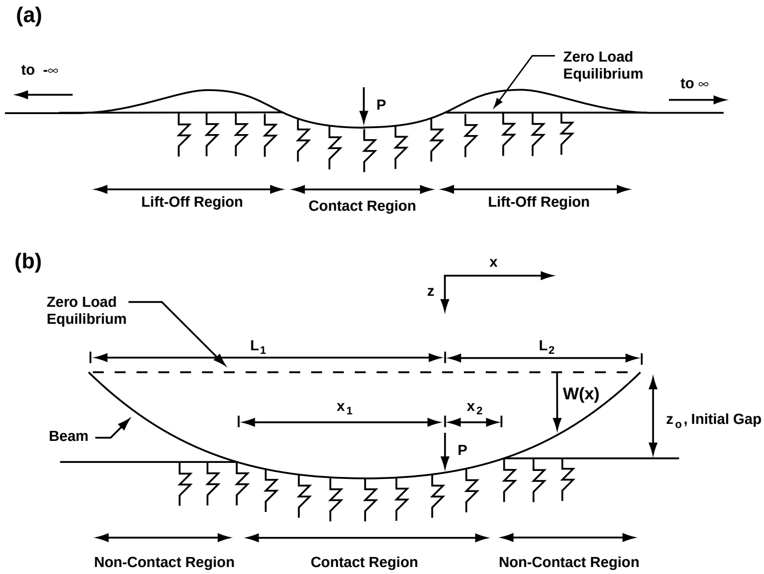

Fig. 1. (a) A schematic of the infinite point loaded beam on a tensionless foundation. (b) A schematic of the finite beam with an eccentric point load and a finite gap.

(1994) introduced a unknown *contact function* that was used in a finite difference scheme to determine the contact area under nonlinear deformations. Alternate solution techniques, such as using boundary elements and finite integral transforms, have also been used with good results (Hu and Hartley, 1994; Dempsey et al., 1984; Dempsey and Hui, 1986; Hui and Dempsey, 1988).

The system under consideration here differs in three fundamental ways from the infinite, symmetric problem described in the early literature. First of all, the beam is finite. This requires specifying some appropriate boundary conditions which, of course, influence the results. Only two cases are considered here: the free–free beam and the pinned–pinned beam. Other boundary conditions will impact the results quantitatively but, from our limited observations, the results will be phenomenologically similar. Hence, other situations are omitted for the sake of brevity. Second, the finite span permits an off-center point load, which breaks the symmetry of the system. Finally, in all cases other than the free–free case, the boundary conditions enable a nonzero gap to exist between the beam and the foundation. All three of these features are built into the mathematical model described in the next section. The upshot is that the general conclusions developed for the infinite problem (i.e., lift-off and fixed contact area) are no longer universally valid. In their place, more diverse phenomena appear, which can be explained in terms of the basic mechanics of the system.

2. Equations of equilibrium and boundary conditions

2.1. Definition of the system

Consider the beam-foundation system shown in Fig. 1b. It consists of an linear elastic Euler–Bernoulli beam and a linear, tensionless foundation. The beam has length L and flexural rigidity EI. An external load P is applied to the beam and the origin of the coordinate system is centered at this load. The distance to the left (right) end of the beam is L_1 (L_2). The contact zone spans the region $-X_1 < X < X_2$. The transverse deflection of the beam is given by $W(x)$. A finite gap Z_o may exist between the foundation and the no-load equilibrium of the beam (given by the dashed line) for all cases except the free–free case. The substrate is a tensionless Winkler foundation with modulus k. Of course, the beam will separate from the foundation once the the displacement is less than the gap size, $W < Z_o$. The one implicit assumption that is made throughout this work is that the load P is always inside the contact zone. Situations where the load is outside of the contact zone do occur for sufficiently large asymmetric loads, particularly when the gap size is very small. The onset of this situation and the ensuing beam response are discussed in Zhang and Murphy (in preparation).

2.2. Equilibrium equations and their solution

The transverse deflection of the neutral axis $W(x)$ is broken into three distinct regions:

$$W(x) = \begin{cases} W_1, & -L_1 < X < -X_1 \\ W_2, & -X_1 < X < X_2 \\ W_3, & X_2 < X < L_2 \end{cases}$$

These correspond to the deflections in the left noncontact region ($W_1 < Z_o$), the contact region ($W_2 \geqslant Z_o$), and the right noncontact region ($W_3 < Z_o$), respectively. Similarly, the equilibrium equation is divided into three parts:

$$\mathrm{EI}\frac{d^4 W_1}{dX^4} = 0, \quad -L_1 < X < -X_1 \tag{1}$$

$$\mathrm{EI}\frac{\mathrm{d}^4W_2}{\mathrm{d}X^4}+k(W_2-Z_\mathrm{o})=P\delta(X),\quad -X_1<X<X_2 \tag{2}$$

$$\mathrm{EI}\frac{\mathrm{d}^4W_3}{\mathrm{d}X^4}=0,\quad X_2<X<L_2 \tag{3}$$

where $\delta(X)$ is Dirac delta function. For convenience, we introduce the quantity $\beta^4=\frac{k}{4\mathrm{EI}}$ along with the following quantities:

$$\xi_1=\beta X_1,\qquad \xi_2=\beta X_2,\qquad l_1=\beta L_1,\qquad l_2=\beta L_2,\qquad l=\beta L,$$
$$z_\mathrm{o}=\beta Z_\mathrm{o},\qquad w=\beta W,\qquad \xi=\beta X,\qquad F=\frac{P}{4\beta^2\mathrm{EI}}$$

Introducing these quantities into the equilibrium equations (Eqs. (1)–(3)) produces the following non-dimensional equations:

$$\frac{\mathrm{d}^4w_1}{\mathrm{d}\xi^4}=0,\quad -l_1<\xi<-\xi_1 \tag{4}$$

$$\frac{\mathrm{d}^4w_2}{\mathrm{d}\xi^4}+w_2-z_\mathrm{o}=F\delta(\xi),\quad -\xi_1<\xi<\xi_2 \tag{5}$$

$$\frac{\mathrm{d}^4w_3}{\mathrm{d}\xi^4}=0,\quad \xi_2<\xi<l_2 \tag{6}$$

The total solutions to Eqs. (4)–(6) are

$$w_1(\xi)=A_1\xi^3+B_1\xi^2+C_1\xi+D_1 \tag{7}$$

$$\begin{aligned}w_2(\xi)=&A_2\cosh(\xi)\sin(\xi)+B_2\cosh(\xi)\cos(\xi)+C_2\sinh(\xi)\sin(\xi)\\&+D_2\sinh(\xi)\cos(\xi)-\frac{F}{2}\sinh|\xi|+\frac{F}{2}\cosh(\xi)\sin|\xi|+z_\mathrm{o}\end{aligned} \tag{8}$$

$$w_3(\xi)=A_3\xi^3+B_3\xi^2+C_3\xi+D_3 \tag{9}$$

Here A_i, B_i, C_i and D_i ($i=1,2,3$) are unknown constants (there are 12). In addition to these constants, the size of the contact zone, given by ξ_1 and ξ_2, is also unknown. Hence, there are a total of 14 unknown constants.

2.3. Boundary conditions

To determine these 14 constants, there must be an equal number of boundary/matching conditions. Lets begin with the matching conditions which occur at the edge of contact. At $\xi=-\xi_1$, ξ_2, the geometric boundary conditions require continuity of the displacement and slope. These are expressed as

$$w_1(-\xi_1)=w_2(-\xi_1),\qquad \frac{\mathrm{d}w_1(-\xi_1)}{\mathrm{d}\xi}=\frac{\mathrm{d}w_2(-\xi_1)}{\mathrm{d}\xi} \tag{10}$$

$$w_2(\xi_2)=w_3(\xi_2),\qquad \frac{\mathrm{d}w_2(\xi_2)}{\mathrm{d}\xi}=\frac{\mathrm{d}w_3(\xi_2)}{\mathrm{d}\xi} \tag{11}$$

There are also four natural boundary conditions at $\xi = -\xi_1,\ \xi_2$. These require continuity of the bending moment and shear force. These are

$$\frac{\mathrm{d}^2 w_1(-\xi_1)}{\mathrm{d}\xi^2} = \frac{\mathrm{d}^2 w_2(-\xi_1)}{\mathrm{d}\xi^2}, \qquad \frac{\mathrm{d}^3 w_1(-\xi_1)}{\mathrm{d}\xi^3} = \frac{\mathrm{d}^3 w_2(-\xi_1)}{\mathrm{d}\xi^3} \tag{12}$$

$$\frac{\mathrm{d}^2 w_2(\xi_2)}{\mathrm{d}\xi^2} = \frac{\mathrm{d}^2 w_3(\xi_2)}{\mathrm{d}\xi^2}, \qquad \frac{\mathrm{d}^3 w_2(\xi_2)}{\mathrm{d}\xi^3} = \frac{\mathrm{d}^3 w_3(\xi_2)}{\mathrm{d}\xi^3} \tag{13}$$

At the edge of the contact zone, it is also evident that the displacement must also equal the gap size. So two additional conditions may be written:

$$w_2(-\xi_1) = z_o, \qquad w_2(\xi_2) = z_o \tag{14}$$

Of course, two alternate conditions that could be used are: $w_1(-\xi_1) = w_3(\xi_2) = z_o$. However, given the matching conditions in Eqs. (10) and (11), these are not statements independent from Eq. (14). Eqs. (10)–(14) give ten conditions. Four additional conditions arise from the boundaries at $\xi = -l_1, l_2$. These will differ, depending on the particular geometry under consideration. Here, two cases are considered. The first is the free–free beam with the boundary conditions:

$$\frac{\mathrm{d}^2 w_1(-l_1)}{\mathrm{d}\xi^2} = 0, \qquad \frac{\mathrm{d}^3 w_1(-l_1)}{\mathrm{d}\xi^3} = 0, \qquad \frac{\mathrm{d}^2 w_3(l_2)}{\mathrm{d}\xi^2} = 0, \qquad \frac{\mathrm{d}^3 w_3(l_2)}{\mathrm{d}\xi^3} = 0 \tag{15}$$

And for the pinned–pinned beam, they are

$$w_1(-l_1) = 0, \qquad \frac{\mathrm{d}^2 w_1(-l_1)}{\mathrm{d}\xi^2} = 0, \qquad w_3(l_2) = 0, \qquad \frac{\mathrm{d}^2 w_3(l_2)}{\mathrm{d}\xi^2} = 0 \tag{16}$$

This leaves 14 boundary/matching conditions to determine the 14 unknown constants, A_i, B_i, C_i, D_i $(i = 1, 2, 3)$, ξ_1 and ξ_2. The boundary conditions are applied to the solutions given in Eqs. (7)–(9) so that the unknowns may be determined. At first glance, this may appear to be a simple, linear boundary value problem. However, because ξ_1 and ξ_2 appear in the argument to the solutions, the problem is nonlinear. Hence, a multi-dimensional Newton Raphson algorithm (Press et al., 1992) is used to obtain the roots to this problem numerically.

2.4. Observations

At this juncture it is worth pointing out some of the similarities and differences from the infinite beam case presented by Weitsman (1970). In that work, Weitsman focused only on the deflection solution in the contacting regime (i.e., w_2). Moreover, because of the symmetry associated with the infinite domain, only even terms are retained in the solution to Eqs. (8). In other words, the terms $\cosh(\xi)\sin(\xi)$ and $\sinh(\xi)\cos(\xi)$ are omitted. This leaves:

$$w_2(x) = B_2\cosh(\xi)\cos(\xi) + C_2\sinh(\xi)\sin(\xi) - \frac{F}{2}\sinh|\xi| + \frac{F}{2}\cosh(\xi)\sin|\xi| \tag{17}$$

Note that z_o is presumed zero. In this case, there are only three unknowns: B_2, C_2, $\xi_1 = \xi_2$ (this last equality is assured by symmetry). These constants are determined through the matching conditions:

$$w_2(\xi_1) = 0, \qquad \frac{\mathrm{d}^2 w_2(\xi_1)}{\mathrm{d}\xi^2} = 0, \qquad \frac{\mathrm{d}^3 w_2(\xi_1)}{\mathrm{d}\xi^2} = 0 \tag{18}$$

The first condition is clear (since $z_o = 0$) and the latter two stems from the fact that there is neither a moment nor a shear force throughout regions one and three (the left and right sides of the beam, outside the contact zone).

What immediate conclusions may be drawn from this problem and how does it differ from the finite problem? First of all, the infinite problem has only three unknowns compared to the 14 for the finite case. The most obvious physical result is that the infinite problem is inherently symmetric. This is evident from the solution form for w_2 and the fact that ξ_1 is presumed equal to ξ_2. What is less obvious is that, after applying the boundary conditions, the contact length, $2\xi_1$, is found to be constant and, hence, is independent of the applied load, see Weitsman (1970). This constant contact length feature leads to a third phenomenon. Namely, as the load is increased the contacting portion of the beam plunges deeper into the foundation but, to enforce the constant contact length requirement, the beam must *lift-off* from the foundation (as is shown schematically in Fig. 1a). And since the constant contact length is assured for any load magnitude, the lift-off phenomenon must also occur for *any* applied load. By contrast, the finite beam problem is not necessarily symmetric, as one would expect if the load were off-center. And, as will be shown in the next section, the contact length is not constant but depends on a number of things. Once this constant contact length requirement is relaxed, the lift-off condition is no longer assured. Of course, given the fact that the finite beam solution contains all of the same terms as the infinite solution (and then some), lift-off is still a possibility—but it is not a requirement.

3. Results

3.1. The free–free beam

In the case of the finite, free–free beam, there can be no initial gap separation, i.e., $z_o = 0$. To examine the differences between the finite and infinite beams, lets begin by considering how the contact length ($\xi_1 + \xi_2$) is influenced by the overall beam length. This is shown in Fig. 2 for the symmetric case ($l_1 = 0.5l$) and for one asymmetric case ($l_1 = 0.6l$). Before proceeding, it should be noted that it was determined numerically that these results are independent of the applied load. Now, consider the symmetric case. For short beam lengths, the contact length scales linearly with the beam length; the slope is one. This simply means that the

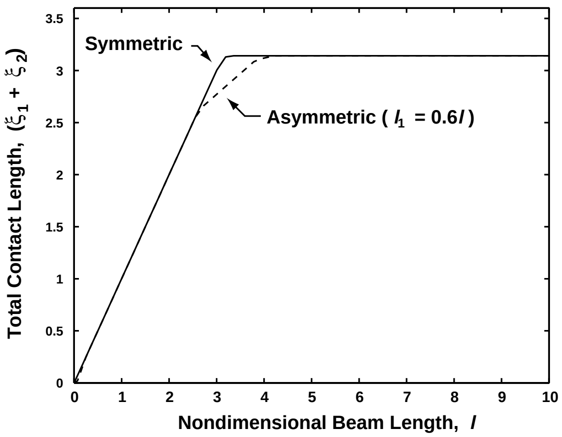

Fig. 2. The total contact length for the free–free beam as a function of the beam length for the symmetric and asymmetric loading scenarios.

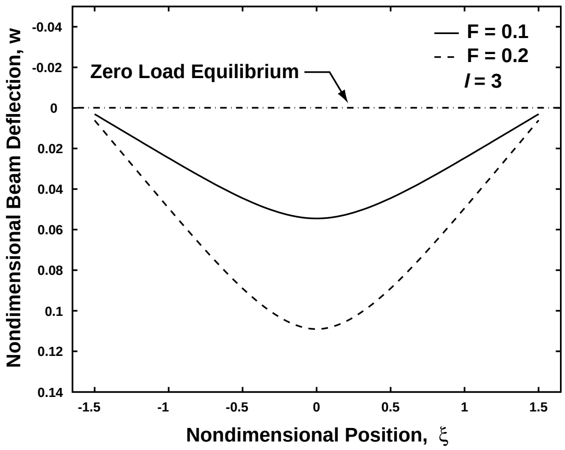

Fig. 3. Deflection shapes for the free–free beam under two different symmetric loads with $l = 3$ and $z_o = 0$. The entire beam is compressed into the foundation; lift-off does not occur.

entire beam is in contact with the foundation. This conclusion is supported by the two deflection curves shown in Fig. 3; the beam subjected to the larger load is compressed further into the substrate. In Fig. 2, as the beam length approaches π, the contact length quickly levels off. With further increases in the beam length, the contact length remains constant at π; this is consistent with the infinite beam case presented by Weitsman (1970). The constant contact length behavior is accompanied by the lift-off phenomenon, as described previously. This is shown in Fig. 4 for a beam length of $l = 4$ with loads $F = 0.1$ and 0.2. From Fig. 4, it is evident that the contact length is independent of load.

For the short beam length regime ($l < \pi$), two mathematical points should be made. The first is that the domain of Eq. (5) is still valid but that the calculated contact length ξ_1 exceeds l_1 (similarly, ξ_2 exceeds l_2). However, the domains of Eqs. (4) and (6) are now incorrect but, since they do not describe any part of the physical beam, this inconsistency is irrelevant. The second is that the displacement constraint condition, Eq. (14), appears to be violated. In fact, this condition is still satisfied—just outside the physical domain,

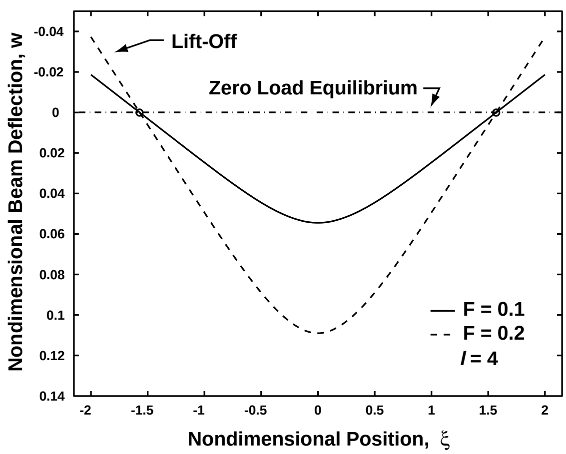

Fig. 4. Deflection shapes for the free–free beam (under the same symmetric loads given in Fig. 3). Here the beam is longer with $l = 4$ and $z_o = 0$. Lift-off has occurred.

$\xi_1 < \xi < \xi_2$. Obviously, this can only happen for a beam with at least one free end, since any boundary support would prevent the end from contacting the foundation.

Fig. 2 also shows an asymmetrically loaded beam with $l_1 = 0.6l$. As in the symmetric case for short beams, the contact length grows linearly (with a slope of one). As before, this means that the entire beam is in contact with the foundation. As the length is increased, the contact length continues to grow, albeit more slowly than the symmetric case. For long beams, the contact length levels off to a value of π, which matches the infinite beam contact length. The more gradual growth of the contact length can be explained by looking at the two distances ξ_1 and ξ_2, which define the edges of contact and are measured from the load location. Fig. 5a and b show the left and right contact lengths, respectively, as a function of the beam length. For small beam lengths, the left side contact length grows linear at a rate of $\xi_1 = 0.6l$ (for this case), which is a faster rate of growth than the symmetric case ($\xi_1 = 0.5l$). As a result, ξ_1 in the asymmetric case will reach the asymptotic value of $\pi/2$ more quickly than its symmetric counterpart, indicating that left side lift-off will occur sooner than in the symmetric case. By contrast, for short beams, the right side contact length grows linearly as $\xi_2 = 0.4l$, which is slower than the symmetric case ($\xi_2 = 0.5l$). Of course, the total contact length is ($\xi_1 + \xi_2$). Hence, the fact that ξ_2 approaches $\pi/2$ more slowly, accounts for why the net contact length for the asymmetric case is below the symmetric case, again see Fig. 2. For confirmation of these interpretations, consider Fig. 6. At a beam length of $l = 3$, Fig. 5a suggests that the left side contact length should be $\xi_1 = \pi/2$ and that left side lift-off should occur. This agrees with Fig. 6. Moreover, by Fig. 5b, the entire right side should be in contact with the substrate and the contact length should be $\xi_2 = 0.4 \times 3 = 1.2$; this also agrees with Fig. 6. For the sake of comparison, the parameter combinations used in Fig. 6 correspond to those used in Fig. 3 (the symmetric case).

3.2. The pinned–pinned beam

In the case of a pinned–pinned beam, two issues are considered. As before, the load may be either symmetric or asymmetric and the gap size may be nonzero. For the moment, lets fix the gap size at $z_o = 0$ and focus on the symmetric and asymmetric loading cases. Fig. 7 shows the contact length as a function of the beam length for the cases $l_1 = 0.5l, 0.6l$. As in the previous section, these results (with $z_o = 0$) were found to be independent of the load magnitude. For short beams, the contact length of the symmetric case

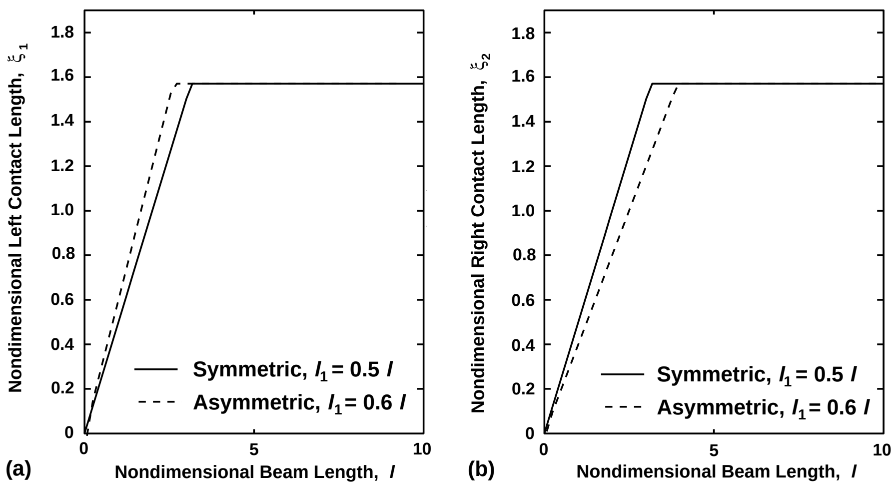

Fig. 5. (a) A comparison of the left side contact length ξ_1 for the symmetric and an asymmetric case in the free–free beam. (b) A similar figure for the right side contact length ξ_2.

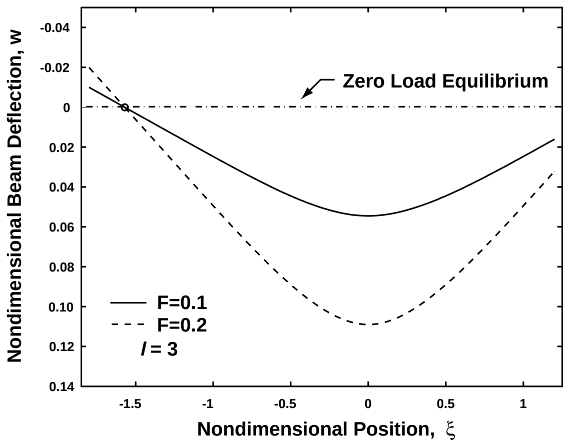

Fig. 6. Deflection curves for the free–free beam under two different loads with $l = 3$. In both cases, one sided lift off clearly occurs, as is predicted for this length beam by Figs. 2 and 5.

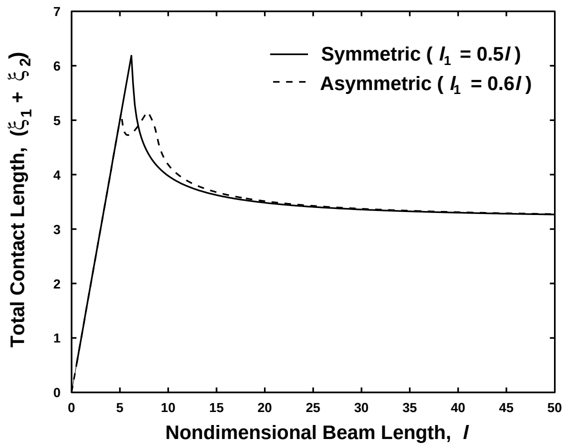

Fig. 7. The total contact length for the pinned–pinned beam as a function of the beam length for the symmetric and asymmetric loading scenarios. The asymmetric case shows multiple peaks due to lift-off of the left and right sides, sequentially.

grows linearly with slope one. Again, this indicates that the entire beam is in contact with the foundation. This persists until $l = 6.187$. As the beam length is increased further, the contact radius actually begins to shrink. This beam length ($l = 6.187$), separating the regions of growing vs. shrinking contact length, is the critical length for the zero gap separation case. The shrinking contact is accomplished by the lift-off phenomenon, which is initiated at the critical beam length. As the beam length is increased further, the contact length decreases and asymptotically approaches π.

The asymmetric loading case in Fig. 7 (for $l_1 = 0.6l$) begins at zero and has a contact length that initially grows linearly with the beam length. Again, in this regime the entire beam is in contact with the foundation. As the length is increased, the contact curve shows two peaks—the contact length grows, shrinks, grows again, and then shrinks again as it asymptotically approaches π. To explain this behavior, consider Fig. 8, which shows the behavior of the two distances ξ_1 and ξ_2 that define the edges of contact. The symmetric

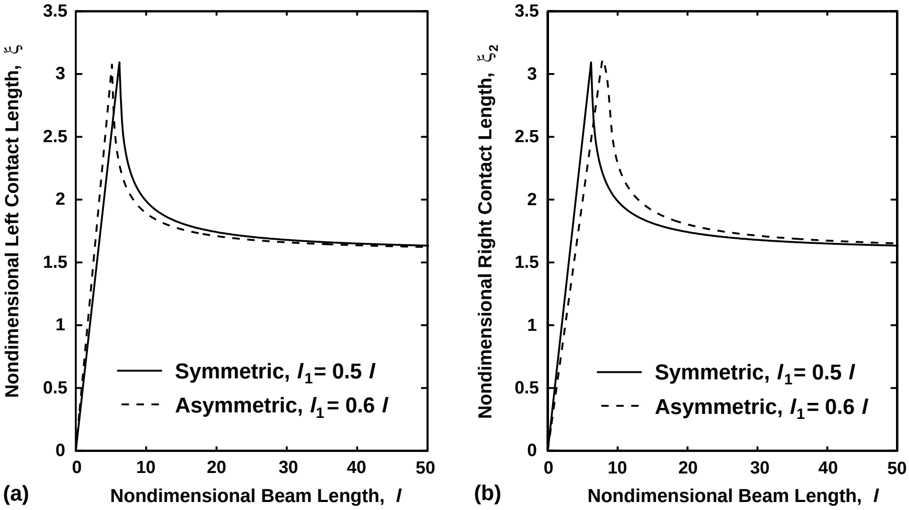

Fig. 8. (a) the left side contact length vs. total beam length for the symmetric and asymmetric case. (b) The right side contact length vs. total beam length for the symmetric and asymmetric case.

case is shown as well, for comparison. As before, left side contact point initially grows as $\xi_1 = 0.6l$. This side of the contact peaks before the symmetric case and then shrinks gradually to the asymptotic value of $\pi/2$. The shrinking contact area (after the peak) occurs because the left side begins to lift-off the foundation. The right side contact initially grows more slowly at $\xi_2 = 0.4l$ and peaks after the symmetric case. The subsequent drop in the contact length is due to right side lift-off. If these two functions are summed, they form the asymmetric case shown in Fig. 7. The first peak is attributed to the peak in ξ_1. The drop in contact results from the drop in ξ_1 after its peak (ξ_2 is increasing but not fast enough to offset the drop in ξ_1). The second peak is due to ξ_2. Finally, Fig. 9 shows the deflection under two different loads, $F = 0.1, 0.2$, for a beam length of $l = 30$. Here both sides have clearly lifted off. Moreover, the contact length, which is very near π, is independent of the applied load.

Now consider the effect of a finite gap separation, z_o. Fig. 10 shows the contact behavior of the symmetric beam both with and without a gap separation. The solid curve shows the contact length with $z_o = 0$ and a load of $F = 0.1$ and 0.5; they are coincident, meaning that the contact length is load independent in the zero gap case. As before, the curve begins at the origin and is nonmonotonic. Now consider a small, nonzero gap separation of $z_o = 0.05$. The contact length is given by the dashed (dash-dotted) line for a load of $F = 0.1$ ($F = 0.5$). These two curves quite clearly show that the contact length is *load dependent* when the gap size is nonzero. An example highlighting the different contact lengths is shown in Fig. 11. Regarding the three cases shown in Fig. 10, three other observations may be made. First, the contact length curve does not begin at the origin as do all the other (zero gap) cases. Contact cannot be initiated until the center point deflection is equal to the gap size – and short beams are too stiff to have this much deflection under a small load. So contact is not initiated until the center point deflection becomes (in dimensional terms) $W(\frac{l}{2}) = Z_o = \frac{PL^3}{48EI}$. With this expression, the appropriate parameter values may be used to determine the critical beam length associated with initial contact. For example, in the case $F = 0.1$ and $z_o = 0.05$, this value is $l = 1.816$, which agrees with the point where the dashed line departs the x-axis in Fig. 10. Second, the curves may or may not increase monotonically, depending on the load level. Third, as the load is increased or as the gap separation decreases, the contact length curve will approach the zero gap result. This suggests, at least heuristically, that the quantity $\frac{F}{z_o}$ would indicate the relative proximity of the nonzero gap

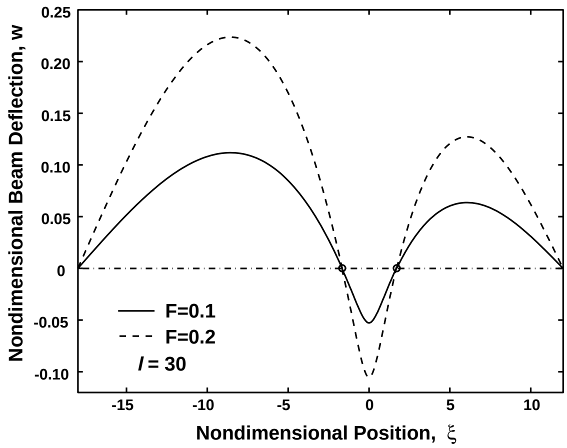

Fig. 9. Deflection curves showing lift-off for the asymmetrically loaded pinned–pinned beam under two different loads. Here, $l = 30$ and $z_o = 0$. Note: the contact length is the same.

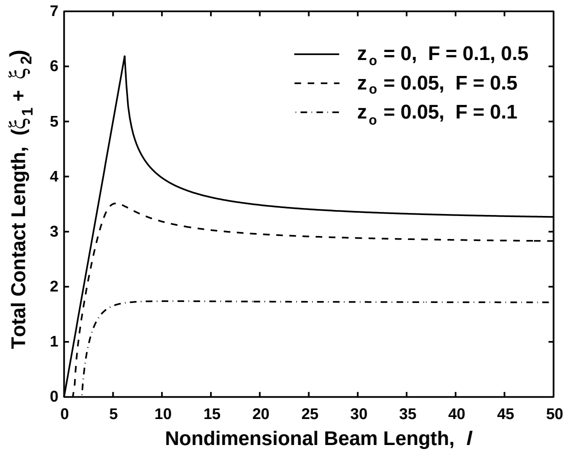

Fig. 10. The total contact length for the symmetrically loaded pinned–pinned beam as a function of the beam length. Several cases are shown—namely, with and without a finite gap separation.

curve to the zero gap curve, large values of F/z_o being closer to the zero gap case. This observation also explains why the zero gap case is independent of the load F ($F/z_o = \infty$, regardless of the load and the curves converge).

Finally, the asymmetric loading case is shown in Fig. 12, where $l_1 = 0.6l$. The no gap case shows the double peak associated with uneven lift-off, as described previously. The introduction of the gap produces similar behavior to the symmetrically loaded case. However, at short beam lengths, the system is sufficiently stiff such that the offset load point does not come into contact with the foundation. This "load outside the zone of contact" situation cannot be captured by this model but may be described by the model in Zhang and Murphy (in preparation).

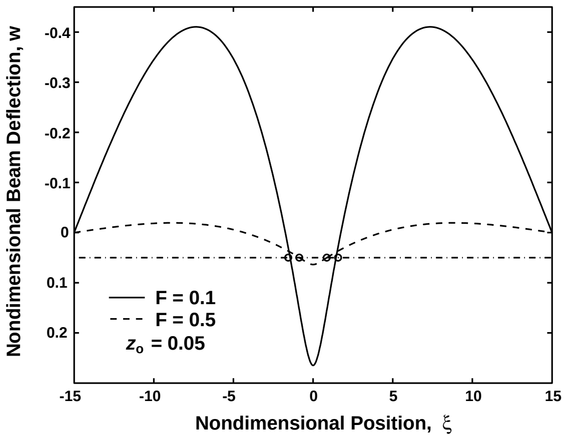

Fig. 11. Deflection curves for the pinned–pinned beam with a finite gap $z_o = 0.05$ under two different symmetric loads. The contact lengths are load dependent in this case.

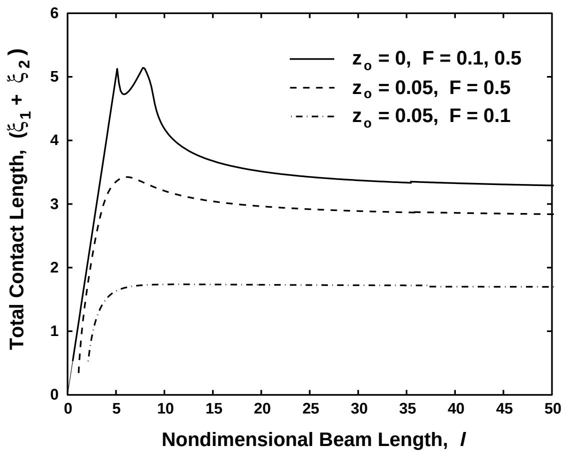

Fig. 12. The total contact length for the asymmetrically loaded pinned–pinned beam as a function of the beam length. These results highlight the influence of a finite gap on the contact length.

4. Conclusions

In situations where adhesion is not significant, the contact problem between a beam and a foundation may be characterized as tensionless. Early studies on tensionless foundations focused on infinite beams whose equilibrium position coincided with the surface of the foundation. The beams were subject to constant lateral point loads and the resulting deformation was examined. It was previously shown that (i) the contact length was constant (i.e., load independent) and equal to π and (ii) the constant contact length was assured by the lift-off phenomenon. These two general results stem from the fact that the beam is infinite, which implies that the load must be centered on the beam (assuring symmetry in the problem). More recent studies have focused on numerical solutions to finite dimensional problems.

In the present study, an analytical approach is taken for a finite beam in contact with a tensionless foundation; this undermines the general results determined above. In the process, it also uncovers a variety of new and interesting behavior. Because the beam is finite, three other issues immediately come into play. Namely, the boundary conditions begin to play a role (though only the free–free and pinned–pinned cases are considered here), the loading may be symmetric or asymmetric, and a finite gap may exist between the beam and the foundation prior to loading. All of these facets influence the contact behavior.

In the case of the free–free beam, where the gap size must be zero, it is shown that the contact length varies with the length of the beam. For short beams, the contact length grows linearly with the beam length. This occurs because the entire beam is in contact with the substrate—so as the beam length increases so does the contact length. Ultimately, as the length increases beyond $l = \pi$, the contact length becomes constant. If the load is shifted off-center, the short beam results are the same. However, as the beam gets longer, the asymmetry permits one sided lift-off and the contact area is less than that for the symmetric case. As the beam length increases, the asymmetry is less relevant and the system approaches the symmetric case.

For the symmetrically loaded pinned–pinned case with zero gap ($z_o = 0$), the contact length initially grows with the beam length until a critical length, after which it begins to shrink. As the beam length is increased further, the contact length asymptotically approaches from above the infinite beam contact length (π). If the load is asymmetric, the contact length goes through a sequence of growing and shrinking: it grows, shrinks, grows again, and shrinks again. The first two parts of this sequence (increasing and then shrinking contact length) is attributed to one sided lift-off and the second two parts occur when the second side lifts-off. As a result, one may conclude that only single or double peak behavior may be seen in these systems (i.e., there is no physical mechanism for a third peak to appear). Finally, as a gap is introduced, $z_o \neq 0$, the contact length becomes load dependent. However, the impact of the gap may be qualitatively assessed by the relative magnitude of the quantity F/z_o. If this quantity is small the contact length (vs. beam length) will be significantly less than the no gap case. If $F/z_o \to \infty$, then the behavior is approaches the no gap case. Moreover, this fact underscores why, in the zero gap case, the contact length is independent of load: $F/z_o = \infty$ is independent of load if $z_o = 0$.

References

Akbarov, S.D., Kocaturk, T., 1997. On the bending of anisotropic (orthotropic) plates resting on elastic foundations that react in compression only. International Journal of Solids and Structures 34, 3673–3689.

Ascione, L., Grimaldi, A., 1984. Unilateral contact between a plate and an elastic foundation. Meccanica 19, 223–233.

Ascione, L., Olivito, R.S., 1985. Unbonded contact of a mindlin plate on an elastic half-space. Meccanica 20, 49–58.

Dempsey, J.P., Hui, L., 1986. Rectangular plates on unilateral edge supports: theory and numerical analysis. Journal of Applied Mechanics 53, 146–150.

Dempsey, J.P. et al., 1984. Contact between plates and unilateral supports. Journal of Applied Mechanics 51, 324–328.

Hetenyi, M., 1946. Beams on Elastic Foundation. University of Michigan Press, Ann Arbor, MI.

Hu, C., Hartley, G.A., 1994. Analysis of a thin plate on an elastic half-space. Computers and Structures 50, 227–235.

Hui, L., Dempsey, J.P., 1988. Unbonded contact of a square plate on an elastic half-space or a winkler foundation. Journal of Applied Mechanics 55, 430–436.

Joo, J.W., Kwak, B.M., 1986. Analysis and applications of elasto-plastic contact problems considering large deformations. Computers and Structures 24, 953–961.

Khathlan, A.A., 1994. Large deformation analysis of plates on unilateral elastic foundation. Journal of Engineering Mechanics 120 (8), 1820–1827.

Lin, L., Adams, G.G., 1987. Beam on tensionless elastic foundation. Journal of Engineering Mechanics 113, 542–553.

Press, W.H., Flannery, B.P., Teukolsky, S.A., Vetterling, W.T., 1992. Numerical Recipies, second ed. Cambridge University Press.

Timoshenko, S.P., 1961. Theory of Elastic Stability, second ed. McGraw-Hill.

Tsai, N.C., Westmann, R.E., 1967. Beams on tensionless foundation. Journal of the Engineering Mechanics 93, 1–12.

Weitsman, Y., 1970. On foundations that reacts in compression only. Journal of Applied Mechanics 37 (7), 1019–1030.

Weitsman, Y., 1971. Onset of separation between a beam and a tensionless elastic foundation under a moving load. International Journal of Mechanical Sciences 13, 707–711.
Weitsman, Y., 1972. A tensionless contact between a beam and an elastic half-space. International Journal of Engineering Science 10, 73–81.
Zhang, Y., Murphy, K.D., in preparation. Contact of a beam with a tensionless foundation resulting from loads outside the region of contact.